IRREGULAR WAVE DEFORMATION

Winyu Rattanapitikon

Department of Civil Engineering, Sirindhorn International Instutute of Technology, Thammasat University, Pathum Thani 12121, Thailand

Tomoya Shibayama

Department of Civil Engineering, Yokohama National University, 79-5 Tokiwadai, Hodogaya-ku, Yokahama 240-8501, Japan

ABSTRACT

A model for irregular wave deformation is developed based on the regular breaking wave model of the authors. Root mean square wave height deformation is computed from the energy flux conservation. The average rate of energy dissipation rate is assumed to be proportional to the difference between the local mean energy flux and stable energy flux. Comparisons are made in the paper with large-scale laboratory data from SUPERTANK project and small-scale laboratory data from Smith and Kraus (1990). Reasonably good agreement is obtained between measured and computed root mean square wave heights. The root mean square relative error of the model is 10.0%

1. INTRODUCTION

In studying many coastal engineering problems it is essential to have accurate information on wave conditions. When waves propagate to the shore, wave profiles are steepen and eventually waves break. Once the waves start to break, energy flux from offshore is dissipated to turbulence and heat and causes the decreasing of wave height towards the shore in the surf zone. Irregular wave breaking is more complex than regular wave breaking. In contrast to regular waves there is no well-defined breaking point for irregular waves. The highest waves tend to break at greatest distances from the shore. Thus, the energy dissipation of irregular waves occurs over a considerably greater area than that of regular waves.

For computing beach transformation, the wave model should be kept as simple as possible because of the frequent updating of wave field for accounting the variability of

mean water surface and the change of bottom profiles. In the present study, wave height transformation will be computed from the energy flux conservation:

$$\frac{\partial(Ec_g)}{\partial x} = -\bar{D}_B \qquad (1)$$

where E is the wave energy density, c_g is the group velocity, x is the distance in cross-shore direction, and $\bar{D}_B$ is the average energy dissipation rate of the breaking waves.

The wave height transformation can be computed from the energy flux balance equation (Eq. 1) by substituting the formula of the average energy dissipation rate, $\bar{D}_B$, and numerical integrating from offshore to shoreline. The main difficulty of energy flux conservation approach is how to determine the average energy dissipation rate, $\bar{D}_B$. Owing to the complexity of wave breaking mechanism, an empirical approach based on measured data is the only feasible way of describing the energy dissipation rate.

In order to make the empirical formula reliable, it is necessary to calibrate or verify that formula with wide range of experimental results. Since many energy dissipation models were developed based on data with the limited experimental conditions, there is still a need for more data to confirm the underlying assumptions and to make the model more reliable. The main target of this study is to develop the energy dissipation model based on wide range of experimental conditions. Small-scale and large-scale experiments have been collected for calibration and verification of the present models. A summary of the collected experimental results is given in Table 1.

The energy dissipation model of irregular breaking wave will be developed based on the same concept as regular breaking wave model of the authors. The summaries of related regular wave models are as follows.

a) Dally *et al.* [1] assumed D_B is proportional to the difference between the local energy flux and the stable energy flux of breaking wave:

$$D_B = \frac{K_d c_g \rho g}{8h}\left[H^2 - (\Gamma h)^2\right] \qquad (2)$$

where all variables are computed based on linear wave theory, K_d is the wave decay factor (=0.15), H is the local wave height, h is the local water depth, Γ is the stable wave factor (=0.4).

b) Rattanapitikon and Shibayama [2] modified the model of Dally *et al.* [1] and proposed to compute the stable wave factor, Γ:

$$\Gamma = \exp\left[-0.36\text{-}1.25\frac{h}{\sqrt{LH}}\right] \qquad (3)$$

where L is the wavelength.

Nine sources of published laboratory results, totally 332 wave profiles, were used to verify the formula.

2. MODEL DEVELOPMENT

Dally [3] used the regular wave model of Dally *et al.* [1] (Eq. 2) to simulate transformation of irregular wave by using wave-by-wave approach. This means that Dally assumed that D_B is proportional to the difference between local energy flux of a breaking wave and stable energy flux. Also, wave-by-wave approach requires much computation time. Therefor it may not be suitable to use in beach deformation model.

However, the model becomes simple if we consider the macro-features by assumption that the average rate of energy dissipation in irregular breaking waves is proportional to the difference between *local mean energy flux* and stable energy flux. After incorporating the fraction of breaking, the average rate of energy dissipation in irregular wave breaking, $\overline{D}_B$, can be expressed as

$$\overline{D}_B = \frac{K_1 Q_b c_g}{h}[E_m - E_s] \tag{4}$$

where

$$E_m = \frac{1}{8}\rho\, gH_{rms}^2 \tag{5}$$

$$E_s = \frac{1}{8}\rho\, gH_s^2 = \frac{1}{8}\rho\, g(\Gamma_{ir}h)^2 \tag{6}$$

in which all variables are computed based on linear wave theory, K_1 is the proportional constant, Q_b is the fraction of breaking waves, c_g is the group velocity related to the peak spectral wave period T_p, E_m is the local mean energy density, E_s is the stable energy flux, H_{rms} is the root mean square wave height, H_s is the stable wave height and Γ_{ir} is the stable wave factor of irregular wave.

Rewriting Eq. (4) in term of wave height:

$$\overline{D}_B = \frac{K_1 Q_b c_g \rho g}{8h}\left[H_{rms}^2 - (\Gamma_{ir}h)^2\right] \tag{7}$$

The stable wave factor, Γ_{ir}, is determined by applying Eq. (3) as

$$\Gamma_{ir} = \exp\left[K_2\,(-0.36-1.25\frac{h}{\sqrt{L_p H_{rms}}})\right] \tag{8}$$

where K_2 is the coefficient, L_p is the wavelength related to the peak spectral wave period.

The local fraction of breaking waves, Q_b, is determined from the derivation of Battjes and Janssen [4] based on the assumption of truncated Rayleigh distribution at the maximum wave height:

$$\frac{1-Q_b}{-\ln Q_b} = \left(\frac{H_{rms}}{H_b}\right)^2 \tag{9}$$

where H_b is the breaking wave height that can be computed by using breaking criteria of Goda [5]:

$$H_b = K_3 L_o\left\{1-\exp\left[-1.5\frac{\pi h}{L_o}\left(1+15m^{4/3}\right)\right]\right\} \tag{10}$$

where K_3 is the coefficient, L_o is the deep-water wavelength, and m is the bottom slope.

Since Eq. (9) is an implicit equation, the iteration process is necessary to compute the fraction of breaking waves, Q_b. It will be more convenient if we can compute Q_b from the explicit form of Eq. (9). From the multi-regression analysis, the explicit form of Q_b can be expressed as the following (with $R^2 = 0.999$):

$$Q_b = 0 \qquad \text{for } \frac{H_{rms}}{H_b} \le 0.43$$

and

$$Q_b = -0.738\left(\frac{H_{rms}}{H_b}\right) - 0.280\left(\frac{H_{rms}}{H_b}\right)^2 + 1.785\left(\frac{H_{rms}}{H_b}\right)^3 + 0.235 \quad \text{for } \frac{H_{rms}}{H_b} > 0.43 \qquad (11)$$

The energy dissipation model (Eqs. 7, 8, 10) contains 3 coefficients, $K_1 - K_3$, that can be found from model calibration.

3. MODEL CALIBRATION

The model is calibrated for determining the optimal values of the coefficients $K_1 - K_3$ in Eqs. (7), (8) and (10). The calibration is carried out with the large-scale experimental data from the SUPERTANK Laboratory Data Collection Project [6]. The SUPERTANK project was conducted to investigate cross-shore hydrodynamic and sediment transport processes. A 76-m-long sandy beach was constructed in a large wave tank of 104 m long, 3.7 m wide, and 4.6 m deep. Wave conditions involved regular and irregular waves. The 20 major tests were performed and each major test consisted of several cases (see Table 2). Most of the major tests were performed under the irregular wave actions, except the test number STBO, STEO, STFO, STGO, STHO, and STIO. The collected experiments for irregular waves include 128 cases of *rms* wave height profiles.

In order to evaluate the accuracy of the prediction, the verification results are presented in term of root mean square (*rms*) relative error, *ER*, which is defined as

$$ER = 100\sqrt{\sum_{i=1}^{tn}(H_{ci} - H_{mi})^2 \Big/ \sum_{i=1}^{tn} H_{mi}^2} \qquad (12)$$

where i is the wave height number, H_{ci} is the computed wave height of number i, H_{mi} is the measured wave height of number i and tn is the total number of measured wave height. Smaller values of *ER* correspond to a better prediction.

The *rms* wave height transformation is computed from the numerical integration of energy flux balance equation (Eq. 1) using the energy dissipation rate $\overline{D}_B$ from Eq. (7):

$$\frac{\partial\left(H_{rms}^2 c_g\right)}{\partial x} = -\frac{K_5 Q_b c_g}{h}\left[H_{rms}^2 - (h\Gamma_{ir})^2\right] \qquad (13)$$

where Γ_{ir} is computed from Eq. (8), Q_b is computed from Eq. (11) and H_b is computed from Eq. (10).

Eq. (13) is solved by backward finite difference scheme. Trial simulations indicated that $K_1 = 0.10$, $K_2 = 1.60$ and $K_3 = 0.10$ give good agreement between measured and computed *rms* wave heights. Finally, the energy dissipation rate of irregular wave breaking can be written as

$$\overline{D}_B = \frac{0.1 Q_b c_g \rho g}{8h}\left[H_{rms}^2 - (\Gamma_{ir} h)^2\right] \qquad (14)$$

where Q_b is computed from Eq. (11)

$$H_b = 0.1 L_o\left\{1 - \exp\left[-1.5\frac{\pi h}{L_o}\left(1 + 15 m^{4/3}\right)\right]\right\} \qquad (15)$$

$$\Gamma_{ir} = \exp\left[-0.58 - 2.0\frac{h}{\sqrt{L_p H_{rms}}}\right] \qquad (16)$$

Comparison between measured and computed *rms* wave heights for all 128 cases is shown in Fig. 1. Table 2 shows the *rms* relative error, *ER*, of the present model for each major tests. The average *rms* relative error, *ER*, for all 128 cases is 9.99% (Table 3) which indicates very well prediction. Typical examples of computed *rms* wave height transformation for each major test are shown in Figs. 2 and 3. From Table 2 and Figs. 2 and 3, it can be seen that the model results generally show very well prediction, except case STKO:s1209b (broad-crested offshore mound) which is shown only fairly well prediction.

4. MODEL VERIFICATION

Since the present model is calibrated with only the data from the large-scale experiments, there is still a need of data from small-scale for confirming ability of the present model. The small-scale experimental data of Smith and Kraus [7] are collected to use in this study. The experiment was conducted to investigate the macro-features of wave breaking over bars and artificial reefs using small wave tank of 45.70-m long, 0.46-m wide, and 0.91-m deep. Both regular and irregular waves were employed in this experiment. Total 12 cases were performed for irregular wave tests. Three irregular wave conditions were generated for each of three bar configurations, as well as for the control case of plane beach.

The wave height transformation is computed from the energy flux balance equation (Eq. 1) using $\overline{D}_B$ from Eq. (14) and numerical integration, using backward finite difference scheme, from offshore to shoreline. All coefficients in the model are kept to be constant for all cases in the verificaiton.

Comparison between measured and computed *rms* wave heights for all cases is shown in Fig. 4. The average *rms* relative error, *ER*, for all cases is 11.23% (Table 3) which indicates a good prediction of the model. Fig. 5 shows the typical examples of computed *rms* wave height transformation for incident *rms* wave height of 10 cm, peak period of 1.75 s and four bottom conditions. The model results generally show good agreement with the measured data. However, the model could not predict the rapid increase and decrease in wave heights near the narrow-crested bar.

5. CONCLUSIONS

A simple model is presented to compute the average rate of energy dissipation in irregular breaking waves. The validity of the model is confirmed by small-scale and large-cale experiments. The average *rms* relative error, *ER*, of the model is 10.0%

ACKNOWLEDGEMENT

The authors wish to express their gratitude to Prof. Yoshimi Goda of the Yokohama National University for his

comments and fruitful discussions. This research was sponsored by the Thailand Research Fund.

REFERENCES

[1] Dally, W.R., Dean, R.G., and Dalrymple, R.A. (1985), Wave height variation across beach of arbitrary profile, J. of Geo. Res., Vol. 90, No. C6, pp. 11917-11927.

[2] Rattanapitikon, W. and Shibayama, T. (1996), Cross-shore sediment transport and beach deformation model, Proc. 25th Coastal Eng. Conf., ASCE, pp. 3062-3075.

[3] Dally, W.R. (1992), Random breaking waves: Field verification of a wave-by-wave algorithm for engineering application, Coastal Engineering, Vol. 16, pp. 369-397.

[4] Battjes, J.A., and Janssen, J.P.E.M. (1978), Energy loss and set-up due to breaking of random waves, Proc. 16th Coastal Engineering Conf., ASCE, pp. 569-587.

[5] Goda, Y. (1970), A synthesis of breaking indices, Trans. Japan Soc. Civil Eng., Vol. 2, Part 2, pp. 227-230.

[6] Kraus, N.C., and Smith, J.M. (1994), SUPERTANK Laboratory Data Collection Project, Technical Report CERC-94-3, U.S. Army Corps of Engineers, Waterways Experiment Station, Vol. 1-2.

[7] Smith, J.M. and Kraus, N.C., (1990), Laboratory study on macro-features of wave braking over bars and artificial reefs, Technical Report CERC-90-12, U.S. Army Corps of Eng., Waterways Exp. Station.

Table 1 Summary of collected experimental data used to validate the present models

No	Sources	Total No. of cases	Bed condition	Apparatus
1	SUPERTANK project [6]	128	sandy beach	large-scale
2	Smith and Kraus [7]	12	plane and barred beach	small-scale
	Total	140		

Table 2 **Root mean square relative error (ER) of the present model comparing with irregular wave data from SUPERTANK project [6]**

Test No.	Description	Total No. of cases	ER. of Present study
ST10	Erosion toward equilibrium, irregular waves	26	5.82
ST20	Acoustic profiler tests, regular and irregular waves	8	6.96
ST30	Accretion toward equilibrium, irregular waves	19	9.99
ST40	Dedicated hydrodynamics, irregular waves	12	10.28
ST50	Dune erosion, Test 1 of 2, irregular waves	8	12.26
ST60	Dune erosion, Test 2 of 2, irregular waves	9	10.03
ST70	Seawall, Test 1 of 3, irregular waves	9	8.21
ST80	Seawall, Test 2 of 3, irregular waves	3	11.03
ST90	Berm flooding, Test 1 of 2, irregular waves	3	4.99
STAO	Foredune erosion, irregular waves	1	5.83
STBO	Dedicated suspended sediment, regular waves	0	-
STCO	Seawall, Test 3 of 3, irregular waves	8	10.21
STDO	Berm flooding, Test 2 of 2, irregular waves	3	13.96
STEO	Laser Doppler velocimeter, Test 1 of 2, regular waves	0	-
STFO	Laser Doppler velocimeter, Test 2 of 2, regular waves	0	-
STGO	Erosion toward equilibrium, regular waves	0	-
STHO	Erosion, transition toward accretion, regular waves	0	-
STIO	Accretion toward equilibrium, regular waves	0	-
STJO	Narrow-crested offshore mound, reg. and irreg. waves	10	11.03
STKO	Broad-crested offshore mound, reg. and irreg. waves	9	23.15
	Total	128	9.99

Table 3 **Root mean square relative error(*ER*) of the present model**

No.	Sources	No. of data set	Present study
1	SUPERTANK project [6]	128	9.99
2	Smith and Kraus [7]	12	11.23
	Total	140	9.99

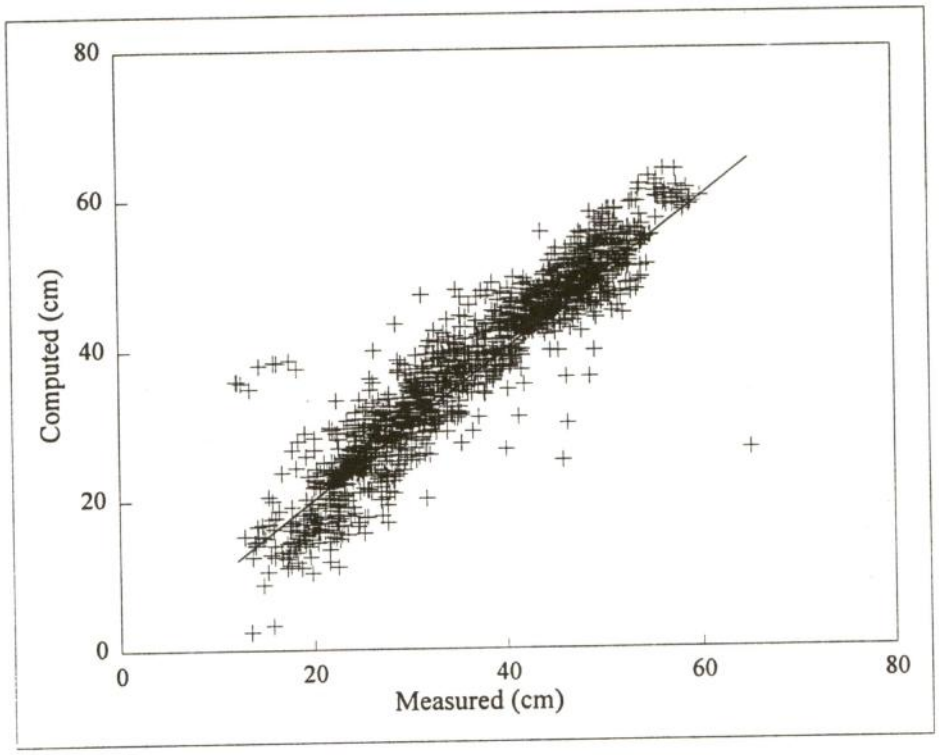

Fig. 1 Comparison between computed and measured *rms* wave height for 128 cases of large-scale experiments (measured data from SUPERTANK project [6])

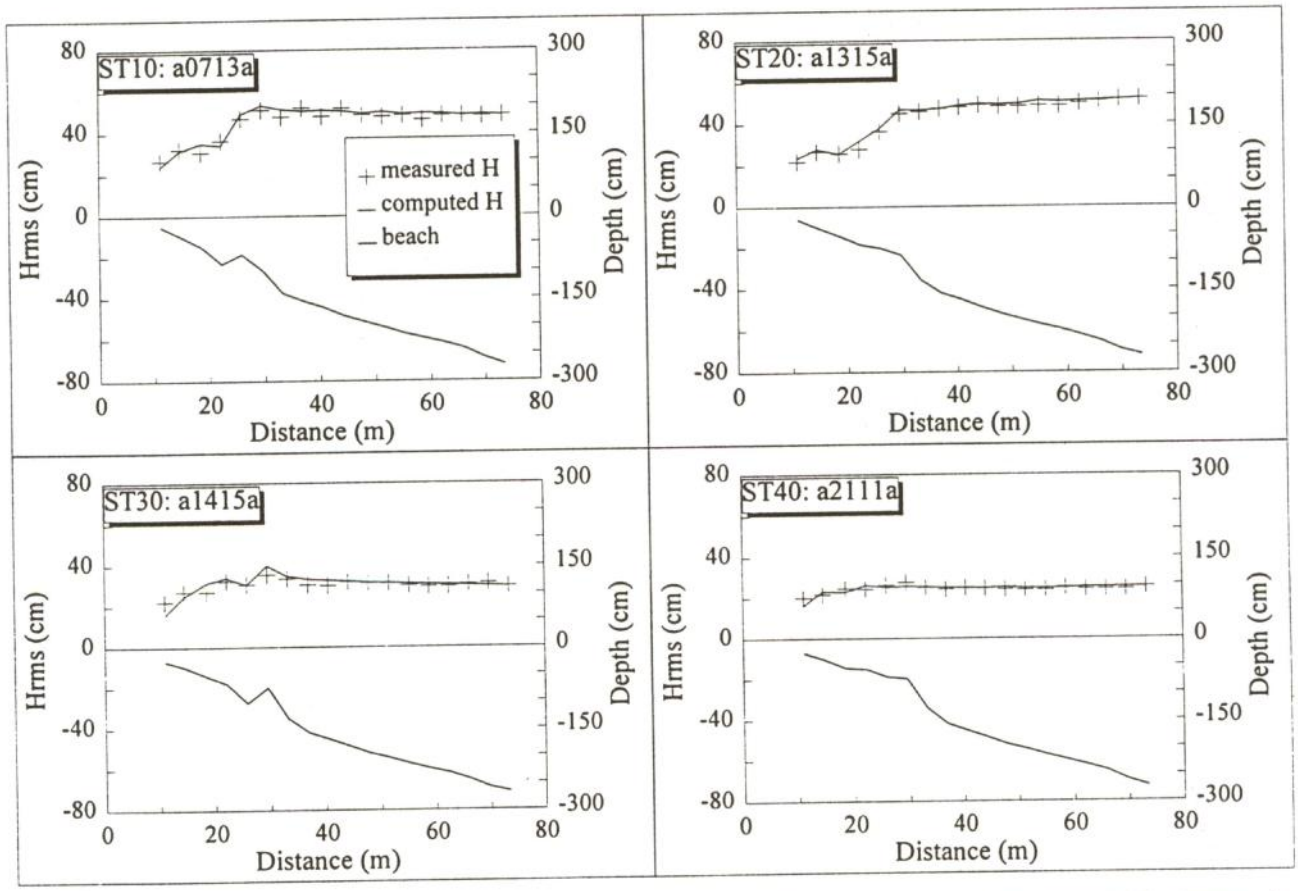

Fig. 2 Examples of computed and measured *rms* wave height transformation for Test No. ST10-ST40 (measured data from SUPERTANK project [6]).

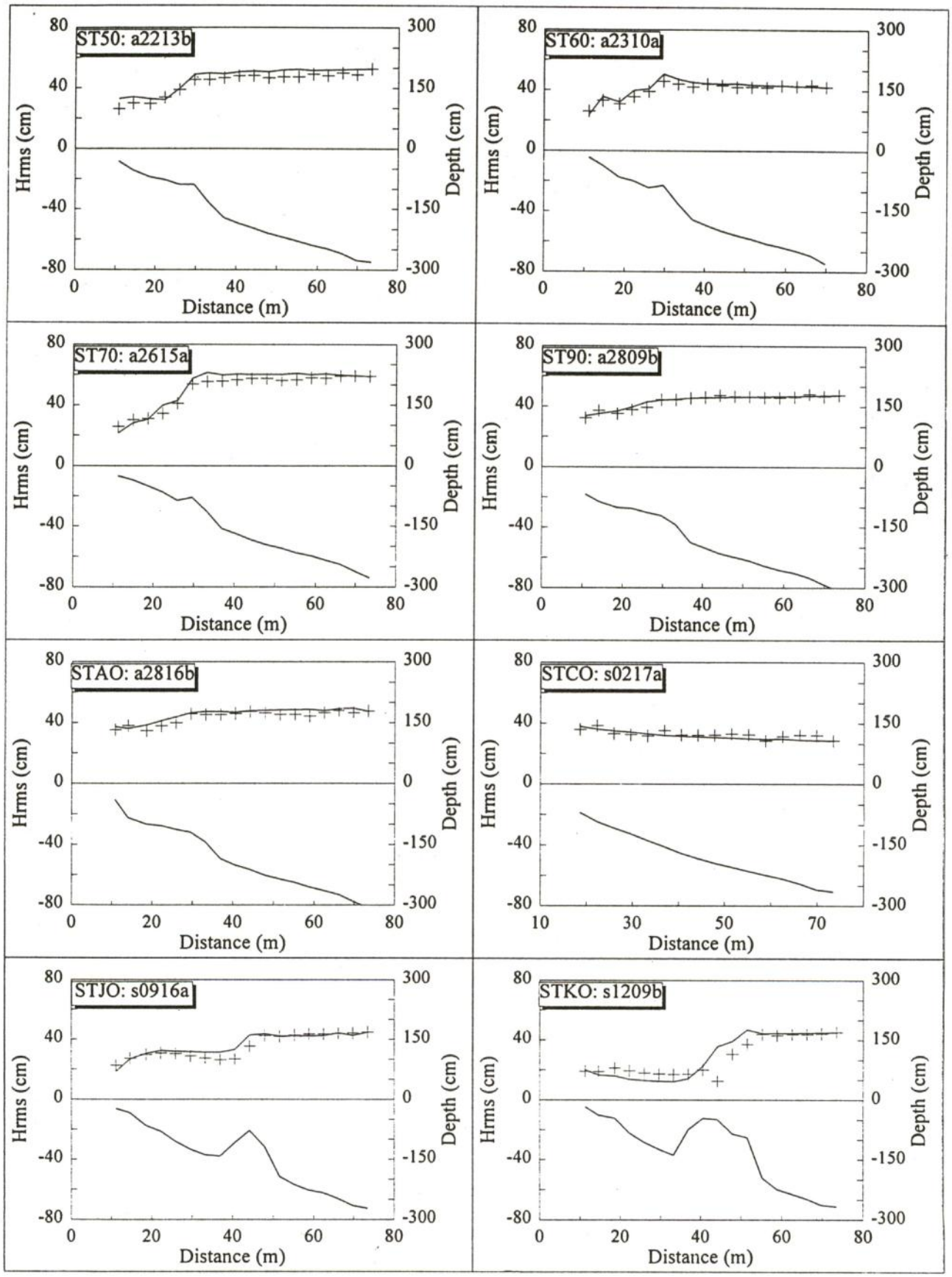

Fig. 3 Examples of computed and measured *rms* wave height transformation for Test No. ST50-STKO (measured data from SUPERTANK project [6])

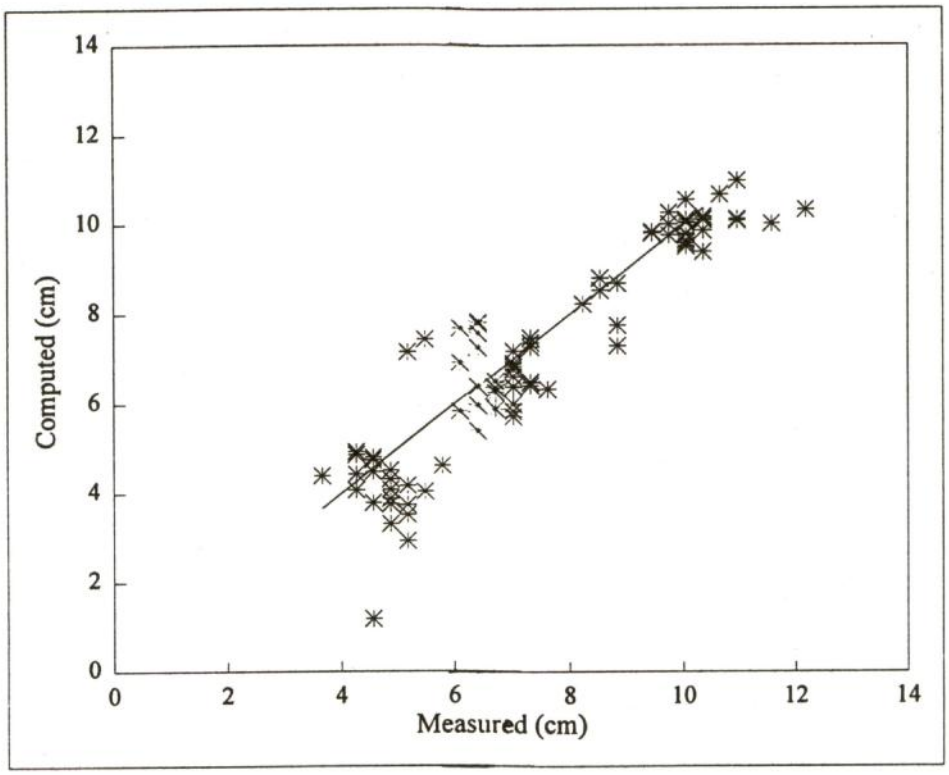

Fig. 4 Comparison between computed and measured *rms* wave height for 12 cases of small-scale experiments (measured data from Smith and Kraus [7])

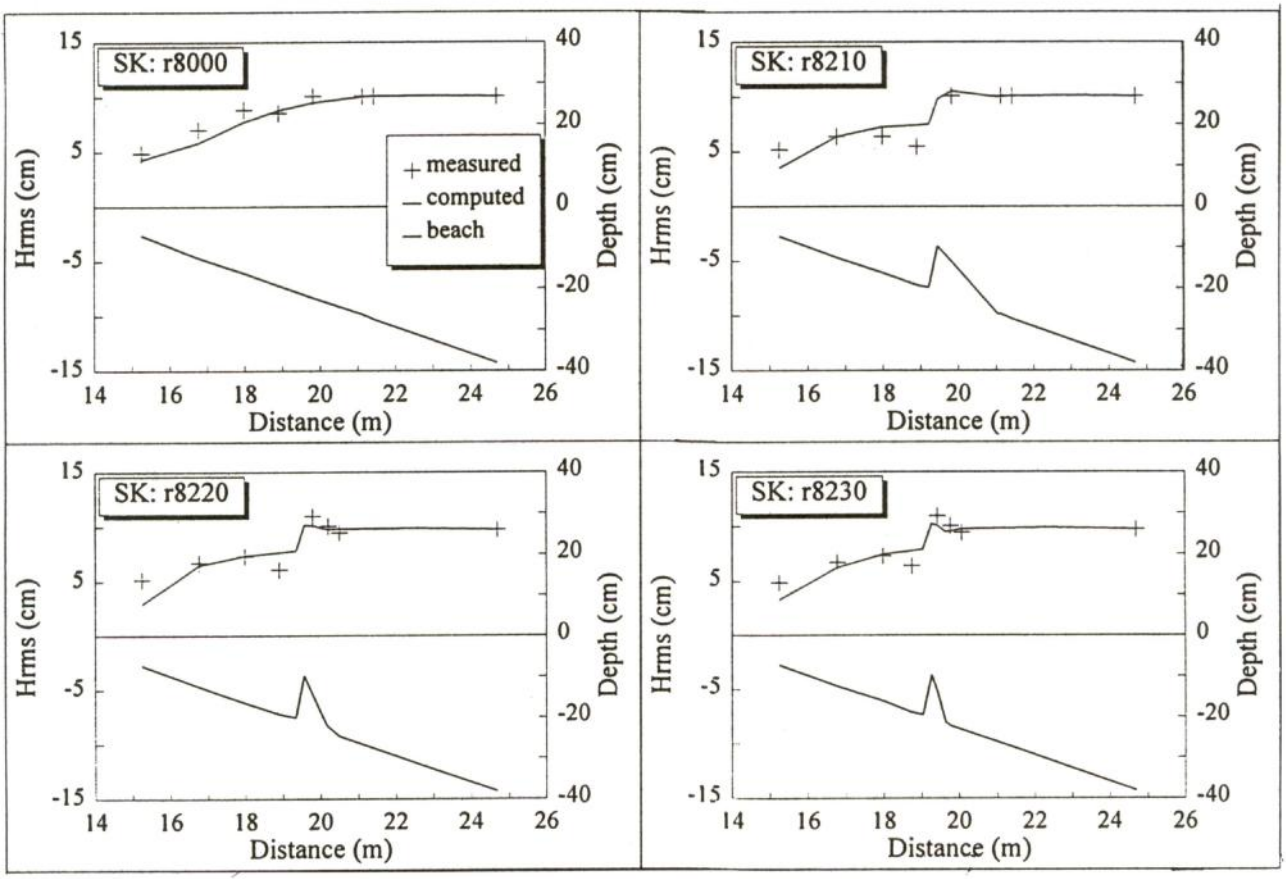

Fig. 5 Examples of computed and measured *rms* wave height for incident *rms* wave height of 10 cm, peak period of 1.75 s, and four bottom conditions (measured data from Smith and Kraus [7])